

## Structural markers observed with endoscopic 3-dimensional optical coherence tomography correlating with Barrett's esophagus radiofrequency ablation treatment response (with videos)

Tsung-Han Tsai, MS,<sup>1</sup> Chao Zhou, PhD,<sup>1</sup> Yuankai K. Tao, PhD,<sup>1</sup> Hsiang-Chieh Lee, MS,<sup>1</sup> Osman O. Ahsen, BS,<sup>1</sup> Marisa Figueiredo, PA,<sup>2,3</sup> Tejas Kirtane, MD,<sup>2,3</sup> Desmond C. Adler, PhD,<sup>4</sup> Joseph M. Schmitt, PhD,<sup>4</sup> Qin Huang, MD,<sup>2,3</sup> James G. Fujimoto, PhD,<sup>1</sup> Hiroshi Mashimo, MD, PhD<sup>2,3</sup>

Boston, Massachusetts, USA

**Background:** Radiofrequency ablation (RFA) is effective for treating Barrett's esophagus (BE) but often involves multiple endoscopy sessions over several months to achieve complete response.

**Objective:** Identify structural markers that correlate with treatment response by using 3-dimensional (3-D) optical coherence tomography (OCT; 3-D OCT).

**Design:** Cross-sectional.

**Setting:** Single teaching hospital.

**Patients:** Thirty-three patients, 32 male and 1 female, with short-segment (<3 cm) BE undergoing RFA treatment.

**Intervention:** Patients were treated with focal RFA, and 3-D OCT was performed at the gastroesophageal junction before and immediately after the RFA treatment. Patients were re-examined with standard endoscopy 6 to 8 weeks later and had biopsies to rule out BE if not visibly evident.

**Main Outcome Measurements:** The thickness of BE epithelium before RFA and the presence of residual gland-like structures immediately after RFA were determined by using 3-D OCT. The presence of BE at follow-up was assessed endoscopically.

**Results:** BE mucosa was significantly thinner in patients who achieved complete eradication of intestinal metaplasia than in patients who did not achieve complete eradication of intestinal metaplasia at follow-up ( $257 \pm 60 \mu\text{m}$  vs  $403 \pm 86 \mu\text{m}$ ;  $P < .0001$ ). A threshold thickness of  $333 \mu\text{m}$  derived from receiver operating characteristic curves corresponded to a 92.3% sensitivity, 85% specificity, and 87.9% accuracy in predicting the presence of BE at follow-up. The presence of OCT-visible glands immediately after RFA also correlated with the presence of residual BE at follow-up (83.3% sensitivity, 95% specificity, 90.6% accuracy).

**Limitations:** Single center, cross-sectional study in which only patients with short-segment BE were examined.

**Conclusion:** Three-dimensional OCT assessment of BE thickness and residual glands during RFA sessions correlated with treatment response. Three-dimensional OCT may predict responses to RFA or aid in making real-time RFA retreatment decisions in the future. (Gastrointest Endosc 2012;76:1104-12.)

(footnotes appear on last page of article)

Radiofrequency ablation (RFA) is an emerging endoscopic therapy for treating Barrett's esophagus (BE).<sup>1-5</sup> By using electrode arrays, RFA catheters deliver radiofrequency energy to the surface of esophageal tissues to ablate BE, with a low stricture rate.<sup>6,7</sup> Recent studies have shown that at 1-year follow-up from the initial RFA treatment, complete eradication of dysplasia (CE-D) was achieved in 90.5% of patients with low-grade dysplasia and in 81% of patients with high-grade dysplasia.<sup>4</sup> At 2-year follow-up, CE-D was achieved in 98% and 93% of

patients with low-grade dysplasia and high-grade dysplasia, respectively.<sup>8</sup> Complete eradication of intestinal metaplasia (CE-IM) was achieved in 93% of patients with dysplasia after 2 years<sup>8</sup> and in 92% of patients with nondysplastic BE at 5-year follow-up.<sup>9</sup> However, recurrence of intestinal metaplasia was observed in 13%<sup>8</sup> and even 25.9%<sup>10</sup> of patients at 1 year after CE-IM was achieved. It is unclear what risk factors are associated with the recurrence of intestinal metaplasia.

Repeated RFA treatments are generally required to achieve complete eradication of aberrant tissues.<sup>11-13</sup> On

average, CE-IM was achieved after 3.4 RFA sessions for patients with nondysplastic BE<sup>9</sup> and over 3.5 sessions for patients with dysplasia.<sup>4,8</sup> Considering the follow-up time between RFA procedures (usually 6-8 weeks), the entire treatment process can easily span half a year or longer. In addition, the cost to achieve complete eradication mounts with each EGD and RFA procedure and has tempered the enthusiasm for treating all nondysplastic BE by using RFA.<sup>14,15</sup> Therefore, improving the effectiveness of each RFA procedure would reduce the number of treatment sessions, improve cost effectiveness, reduce patient anxiety, and make this therapy available to a wider patient population.

Optical coherence tomography (OCT) is a volumetric imaging technique that generates cross-sectional and 3-dimensional (3-D) images of tissue microstructures, with micron scale resolution.<sup>16</sup> Endoscopic OCT techniques have been developed to image the human GI tract, with over 1 mm imaging depth.<sup>17-26</sup> Two-dimensional OCT has been used to evaluate specialized intestinal metaplasia, dysplasia, and adenocarcinoma in the esophagus and has achieved a high sensitivity and specificity for differentiating different pathologies.<sup>22,27</sup> Recently, endoscopic 3-D OCT has become possible because of dramatic increases in imaging speed.<sup>23-26</sup> Three-dimensional OCT provides a powerful combination of high resolution, large field of view, and rapid data acquisition. Three-dimensional OCT has been used to image patients with upper and lower GI diseases.<sup>23,26</sup> Recent studies demonstrated that 3-D OCT can identify buried glands before and after CE-IM from RFA treatment.<sup>23,28</sup> The objective of this investigation was to identify possible structural markers that predict RFA treatment response by using endoscopic 3-D OCT.

## METHODS

### Patient enrollment and study protocol

This study was conducted at the Veterans Affairs Boston Healthcare System, Jamaica Plain Campus, over the past 2 years. The study protocol was approved by the Veterans Affairs Boston Healthcare System, Harvard Medical School, and the Massachusetts Institute of Technology. Patients were diagnosed with standard white light endoscopy, and the length of visible BE was recorded based on the Prague C&M criteria.<sup>29</sup> Thirty-three patients with short-segment (<3 cm) BE, including one woman, were recruited for this study. The study also included patients who initially presented with long-segment BE that was reduced to <3 cm segment by prior circumferential RFA treatment by using the BARRX Halo360 catheter (Covidien, Sunnyvale, CA). Informed consent was obtained from each patient. Only patients with short-segment BE were imaged in order to ensure consistent OCT imaging catheter placement at the gastroesophageal junction (GEJ) and ascertaining the presence of BE, its thickness, and the presence of residual glands relative to the GEJ within the

### Take-home Message

- Three-dimensional optical coherence tomography provides a useful tool for identifying factors associated with radiofrequency ablation treatment response and may improve the effectiveness of therapy to reduce the number of treatments required to achieve complete response in the future.

OCT pullback image. This study focused on patients receiving ablation with the Halo90 catheter. For each RFA treatment, the patient received two sets of ablations that were done with the BARRX Halo90 catheter (300 W at 12 J/cm<sup>2</sup> for each set of ablations), with rigorous scraping to remove desquamated epithelium between the two ablations, per standard protocol set by the manufacture. Patients with circumferential short-segment BE also were treated with the Halo90 catheter in order to maintain a consistent procedure and ablation energy level. After the RFA, patients were treated with a proton pump inhibitor, that is, 40 mg of esomeprazole or omeprazole twice daily. At 6 to 8 weeks follow-up, the presence of residual BE was evaluated by using white light endoscopy and narrow-band imaging as well as random 4-quadrant pinch biopsies. If no visible BE was observed endoscopically, and no intestinal metaplasia was found from biopsies at the GEJ, the patient was classified as CE-IM. There were 13 patient in the CE-IM group and 20 patients in the non-CE-IM group in this study.

### Endoscopic 3-D OCT imaging

A prototype endoscopic 3-D OCT system,<sup>25,30</sup> developed by LightLab Imaging, St. Jude Medical (Westford, Mass), was used for this study. The system had a lateral resolution of 15  $\mu$ m, an axial resolution of 5  $\mu$ m, and an imaging depth of about 2 mm in tissue. Three-dimensional OCT imaging was performed with the OCT catheter introduced through the biopsy channel of the endoscope (GIF Q180; Olympus, Tokyo, Japan), enabling simultaneous video endoscopy. Volumetric OCT data were acquired at 60,000 axial lines per second and 60 frames per second. The imaging catheter scanned a helical pullback pattern with an 8-mm circumference and 20-mm pullback length within 20 seconds. The endoscope was at the neutral position, with the imaging catheter placed at 6 o'clock in the endoscopic field. The imaging catheter was in contact with the esophagus, and the pullback imaging spanned the GEJ. The esophagus was deflated and naturally wrapped around the OCT catheter during imaging acquisition to maintain a consistent catheter contact for all patients. Multiple 3-D OCT datasets were acquired at the GEJ before and immediately after the RFA treatment.

## Image analysis

Each 3-D OCT data set was reviewed and analyzed by using 3-D rendering software (Amira; Visage Imaging, Inc., San Diego, CA). The BE epithelium thickness was measured from cross-sectional OCT images obtained before the RFA treatment. As indicated in Figure 1, the BE thickness was measured as the vertical distance from the top of the lamina propria/muscularis mucosa layer to the surface of the BE epithelium at the center position where the OCT catheter had the best contact with the esophagus. Multiple BE thickness measurements were obtained from each 3-D data set every 1 mm along the entire BE length. The average and maximum BE thickness were recorded for each patient for statistical comparison between the CE-IM and non-CE-IM groups.

In addition, two types of residual glandular structures were observed by reviewing 3-D OCT images obtained immediately after the second RFA. The first type of glandular structure was unburned BE epithelium that was likely missed by RFA and showed an epithelial structure similar to that of regular BE. The second type of glandular structure consisted of hyposcattering glandular structures above the lamina propria/muscularis mucosa layer at the RFA treatment site, representing residual glands. The presence or absence of these residual glands was recorded for each patient.

## Statistical analysis

The primary study outcome was to determine the accuracy of using BE thickness measured with OCT before RFA to predict the treatment response (presence or absence of endoscopically visible residual BE at follow-up). A *t* test was used to compare the average and maximum BE thickness from the CE-IM and non-CE-IM groups. To evaluate whether BE thickness can be used to predict the RFA treatment response, receiver operating characteristic curves were plotted by using a discrimination threshold ranging from 100  $\mu\text{m}$  to 800  $\mu\text{m}$  for average and maximum BE thickness, respectively. A decision threshold was determined from the receiver operating characteristic curves to achieve maximum overall accuracy. Sensitivity, specificity, positive predictive value, negative predictive value, and accuracy of the prediction were then calculated.

The secondary study outcome was to evaluate the correlation between the presence or absence of residual glands on OCT imaging immediately after RFA versus RFA treatment response assessed endoscopically on follow-up. We also evaluated the correlation between the BE thickness before RFA versus the presence or absence of residual glands immediately after RFA. The sensitivity, specificity, positive predictive value, negative predictive value, and accuracy were calculated.

All statistical analyses were performed by using MATLAB software (Mathworks Inc., Natick, MA). All tests were 2-sided, and a *P* value of  $< .05$  was considered statistically significant.

## RESULTS

Table 1 lists demographic information of the patients enrolled in this study. The average age for the CE-IM and non-CE-IM groups was comparable ( $P = .86$ ). The CE-IM group consisted of 13 patients (4 patients had BE without dysplasia, 2 BE with low-grade dysplasia, and 7 BE with high-grade dysplasia at presentation). The non-CE-IM group consisted of 20 patients (10 patients had BE without dysplasia, 4 BE with low-grade dysplasia, and 6 BE with high-grade dysplasia at presentation). Patients in the non-CE-IM group are presumed to eventually have a treatment response with additional RFA treatments and convert to the CE-IM group, and investigation of this group is ongoing. The number of prior RFA treatments and the length of BE was not statistically different between the two groups. There were no adverse events after RFA treatment.

Figure 1A shows an endoscopic image of the GEJ before focal RFA treatment was applied. Three-dimensional OCT imaging was performed at the GEJ over the area of BE (pink). Figure 1B shows a representative cross-sectional OCT image obtained at the GEJ before the RFA treatment, together with histology obtained from the same site (Fig. 1C). The thickness of the BE epithelium was measured from the OCT image as distance between the BE surface to the top of the lamina propria/muscularis mucosa layer.

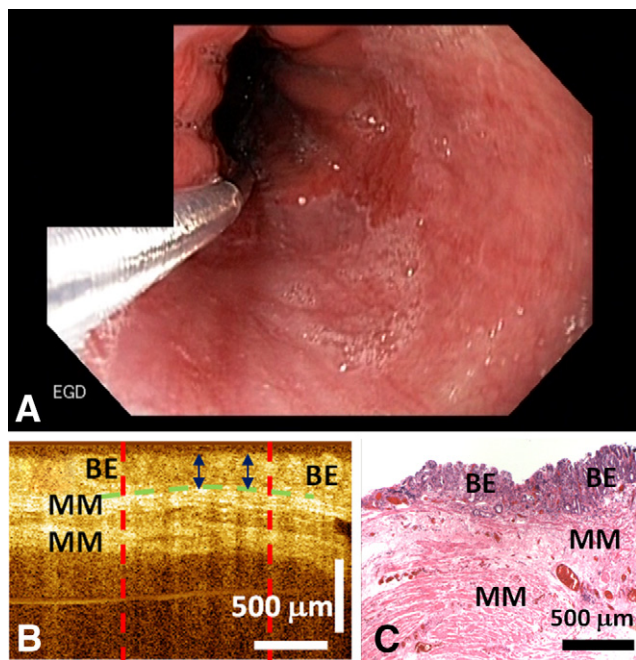


**Figure 1.** **A**, Representative endoscopic image of the gastroesophageal junction before radiofrequency ablation treatment. **B**, Representative cross-sectional optical coherence tomography image. **C**, Corresponding histology illustrating the Barrett's esophagus epithelium thickness measurement (H&E, orig. mag.  $\times 4$ ). BE, Barrett's esophagus; MM, muscularis mucosa.



**TABLE 1. Patient demographic information**

	CE-IM group	Non-CE-IM group	P value
Enrollment, no.	13	20	
Sex, male/female, no.	12/1	20/0	
Age, mean (SD), range, y	64.9 (7.7) 51-77	65.6 (15.8) 33-92	.86
Initial diagnosis, no.			
BE w/o dysplasia	4	10	
Low-grade dysplasia	2	4	
High-grade dysplasia	7	6	
Prior RFA treatments, mean (SD), range	2.4 (1.9) 0-7	1.7 (1.6) 0-6	.34
Length of BE, mean (SD), range, cm	1.3 (0.8) 0.5-3	1.0 (0.7) 0.5-3	.29

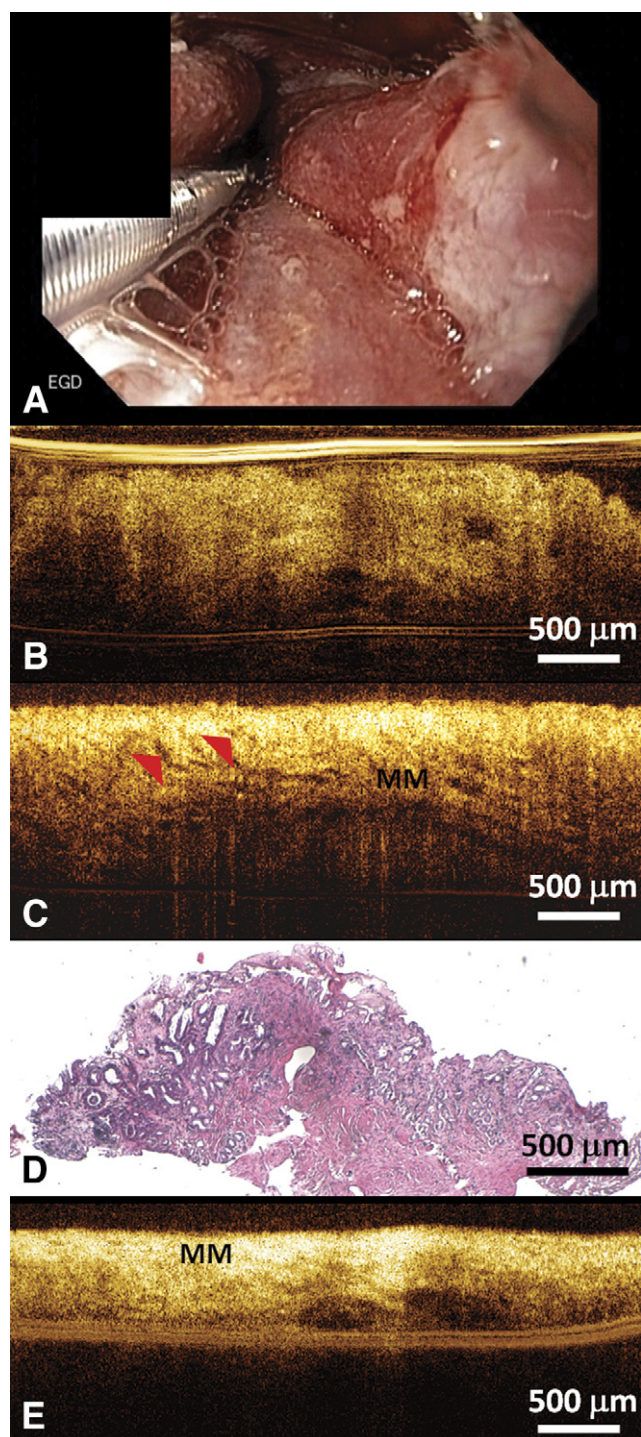
CE-IM, Complete eradication of intestinal metaplasia; SD, standard deviation; BE, Barrett's esophagus; RFA, radiofrequency ablation.

Figure 2A shows an endoscopic image of the GEJ immediately after focal RFA treatment with scraping to remove desquamated epithelium between first and second RFA applications. The RFA-treated area was covered with blood and burned tissue, making it difficult to identify residual BE patches on white light endoscopy or narrow-band imaging. Figure 2B shows a representative cross-sectional OCT image obtained immediately after RFA. A similar epithelium structure was observed compared with Figure 1B, indicating the presence of residual BE that was missed by the RFA treatment. A video of cross-sectional OCT images scanning through the unburned BE area is provided in the supplemental materials (Video 1, available online at [www.giejournal.org](http://www.giejournal.org)). Another type of residual glandular structure usually can be observed after insufficient power delivery on the tissue, leading to hyposcattering features above the lamina propria/muscularis mucosa layer at the RFA-treated site in OCT images. Figure 2C shows residual glands (*red arrows*) above the muscularis mucosa layer, suggesting that these glands were not effectively removed by the RFA treatment. A biopsy was taken from the same site immediately after the OCT imaging and confirmed the presence of residual BE glands immediately after the RFA treatment (Fig. 2D). A video of cross-sectional OCT images scanning through these residual BE glands is provided in the supplemental materials (Video 2, available online at [www.giejournal.org](http://www.giejournal.org)). Figure 2E shows a representative OCT image demonstrating effective RFA treatment, where the muscularis mucosa layer was on top of the tissue surface with no epithelial structures above it. A video of cross-sectional OCT images scanning through the effectively treated area is provided in the supplemental materials (Video 3, available online at [www.giejournal.org](http://www.giejournal.org)).

The BE thickness measured with OCT before RFA was found to be a predictor of the RFA treatment response. Both the average and maximum BE thickness before RFA were significantly thinner for the CE-IM group compared

with the non-CE-IM group (average BE thickness,  $257 \pm 60 \mu\text{m}$  versus  $403 \pm 86 \mu\text{m}$ ;  $P < .0001$ ; maximum BE thickness,  $293 \pm 64 \mu\text{m}$  versus  $471 \pm 107 \mu\text{m}$ ;  $P < .0001$ ). The scatter plot in Figure 3A shows the difference between the average BE thickness for the two groups. Figure 3B shows receiver operating characteristic curves in which average and maximum BE thickness were used to predict RFA treatment response. The area under the curve was 0.942 ( $P < .001$ ) and 0.934 ( $P < .001$ ) using the average and maximum BE thickness, respectively. An average BE thickness of  $333 \mu\text{m}$  was determined from the receiver operating characteristic curve to achieve the best prediction accuracy. By using this decision threshold, a sensitivity of 92.3% (12/13), specificity of 85% (17/20), positive predictive value of 80%, negative predictive value of 94.4%, and an accuracy of 87.9% (29/33) were obtained for predicting treatment response evaluated by the presence or absence of endoscopically visible residual BE at follow-up visit by using the average BE thickness measured with OCT before the RFA treatment (Table 2). Considering only the patients with dysplastic BE (19/33), a sensitivity of 100% (9/9), specificity of 90% (9/10), positive predictive value of 90%, negative predictive value of 100%, and accuracy of 94.7% (18/19) were obtained for predicting treatment response evaluated by the presence or absence of endoscopically visible residual BE at the follow-up visit by using the average BE thickness measured with OCT before RFA treatment. The BE thickness measured with OCT was not correlated with the length of the BE ( $P = .88$ ) or the number of prior RFA treatments ( $P = .24$ ).

A BE thickness of over  $333 \mu\text{m}$  also was found to correlate with the presence of residual glands immediately after RFA (Table 3; sensitivity 91.7% [11/12], specificity 85% [17/20], positive predictive value 78.6%, negative predictive value 94.4%, and accuracy 87.5% [28/32]). Note that one patient was excluded from this analysis due to the lack of OCT images immediately after RFA. Finally, the pres-



**Figure 2.** **A**, Representative endoscopic image of the gastroesophageal junction immediately after radiofrequency ablation (RFA) treatment. **B**, Representative cross-sectional optical coherence tomography (OCT) image showing unburned Barrett's esophagus epithelium missed by RFA. **C**, Representative cross-sectional OCT image showing residual glands after RFA. **D**, Corresponding histology of representative cross-sectional OCT image confirming residual BE glands after RFA (H&E, orig. mag. x4). **E**, Representative cross-sectional OCT image showing effective RFA treatment. The entire BE epithelium was ablated, resulting in exposed muscularis mucosa on the surface. OCT, optical coherence tomography; MM, muscularis mucosa.

ence of residual glands observed with OCT immediately after RFA was found to be another predictor of the RFA treatment response (Table 4). Sensitivity of 83.3% (10/12), specificity of 95% (19/20), positive predictive value of 90.9%, negative predictive value of 90.5%, and accuracy of 90.6% (29/32) were achieved by using the presence of residual glands visible on OCT immediately after RFA to predict the presence of endoscopically visible residual BE at follow-up.

## DISCUSSION

Although endoscopic 3-D OCT does not have the same magnification or contrast as conventional histopathology, it can visualize tissue microstructure in vivo over a large field of view and provides real-time, depth-resolved information with micron scale resolution. Each 3-D OCT dataset in our study covers about 160 mm<sup>2</sup> in the distal esophagus. Although this is only a fraction of the field observed with white light endoscopy, it is many times larger than the field covered by pinch biopsy, and 3-D OCT provides complementary information about BE thickness as well as tissue morphology. This is especially important immediately after the RFA treatment, when the endoscopic imaging field is covered with blood and tissue debris. Because of the limited visibility immediately after the RFA treatment, it is difficult to evaluate the presence of residual glands or unburned BE by using white light endoscopy or narrow-band imaging. Similarly, imaging modalities that require contrast agents such as confocal endomicroscopy have limited use because extravasation of the contrast material obliterates the viewing area after RFA. However, as demonstrated, residual glandular structures can be observed by using 3-D OCT.

In this study, 3-D OCT identified structural markers, including the thickness of the BE epithelium before RFA and the presence of residual glands immediately after RFA, which might be used to predict RFA treatment response at follow-up with high accuracy. We found that patients with an average BE thickness of over 333 μm were likely to have endoscopically visible residual BE at the follow-up visit 6 to 8 weeks after the RFA treatment. This result was not surprising, however, because the dosage of the RFA treatment has been set to achieve best efficacy with minimum injury depth.<sup>6,31</sup> The energy delivery of a standard RFA application might not reach deep enough when the BE epithelium is thick. There are other possible confounding variables that may contribute to depth variation or incompleteness of the ablation, including variation of the RFA electrode contact with the esophagus and coagulated/sloughing debris building up on the electrode surface with repeated ablations in a patient.<sup>31</sup> Indeed, we found a correlation between the BE epithelium thickness and the presence of residual glands immediately after RFA, suggesting that not all RFA applications were effective. Insufficient energy delivery at the treatment sites or leaving BE

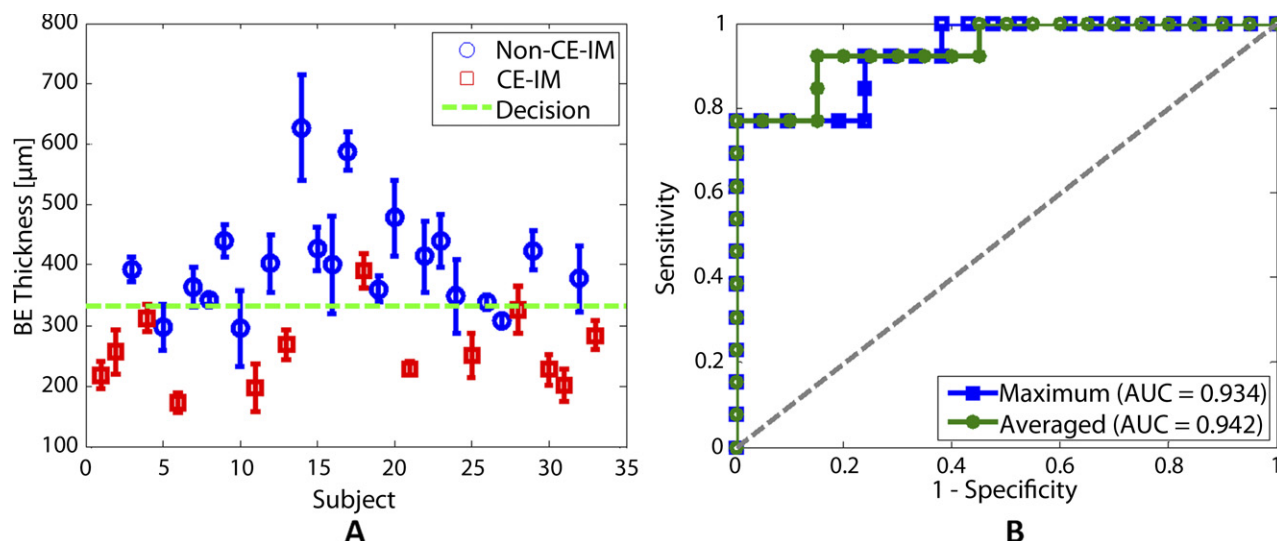


**Figure 3.** **A**, Scatter plot of the average Barrett's esophagus (BE) epithelium thickness measured by optical coherence tomography. *Blue circles*: non-complete eradication of intestinal metaplasia group; *Red crosses*: complete eradication of intestinal metaplasia group; *Green dotted line*: discrimination threshold at 333  $\mu\text{m}$  as determined from the average BE thickness receiver operating characteristic (ROC) curve in (**B**). **B**, ROC curves of treatment response prediction by using average (*green*) and maximum (*blue*) BE thickness. The area under the curve values were 0.942 ( $P < .001$ ) and 0.934 ( $P < .001$ ) by using the average and maximum BE thicknesses, respectively. *BE*, Barrett's esophagus; *CE-IM*, complete eradication of intestinal metaplasia; *AUC*, area under the curve.

**TABLE 2. Average BE thickness measured by OCT before RFA predicts the presence or absence of endoscopically visible residual BE at follow-up visit**

	Absence of residual BE at follow-up	Presence of residual BE at follow-up	Total	
Average BE thickness $< 333 \mu\text{m}$	12	3	15	PPV 80%
Average BE thickness $\geq 333 \mu\text{m}$	1	17	18	NPV 94.4%
Total	13	20	33	
Sensitivity 92.3%		Specificity 85%	Accuracy 87.9%	

*BE*, Barrett's esophagus; *OCT*, optical coherence tomography; *RFA*, radiofrequency ablation; *PPV*, positive predictive value; *NPV*, negative predictive value.

**TABLE 3. Average BE thickness measured by OCT before RFA predicts the presence or absence of residual glands measured by OCT immediately after RFA**

	Absence of residual glands immediately after RFA	Presence of residual glands immediately after RFA	Total	
Average BE thickness $< 333 \mu\text{m}$	11	3	14	PPV 78.6%
Average BE thickness $\geq 333 \mu\text{m}$	1	17	18	NPV 94.4%
Total	12	20	32	
Sensitivity 91.7%		Specificity 85%	Accuracy 87.5%	

*BE*, Barrett's esophagus; *OCT*, optical coherence tomography; *RFA*, radiofrequency ablation; *PPV*, positive predictive value; *NPV*, negative predictive value.

unburned may be factors that lead to endoscopically visible residual BE at follow-up.

The efficacy of ablation therapies is generally assessed by follow-up endoscopy 6 to 8 weeks after RFA,<sup>11-13</sup> and patients undergo repeated ablation if residual BE is ob-

served. Our results suggest that the patient response rate may be stratified based on the BE thickness measured before RFA. By using this structural marker, it may be possible to adjust RFA treatment for each patient to optimize response. For patients with thicker BE epithelium, a



**TABLE 4. Presence or absence of residual glands measured by OCT immediately after RFA predicts the presence or absence of endoscopically visible residual BE at follow-up visit**

	Absence of residual BE at follow-up	Presence of residual BE at follow-up	Total	
Absence of residual glands immediately after RFA	10	1	11	PPV 90.9%
Presence of residual glands immediately after RFA	2	19	21	NPV 90.5%
Total	12	20	32	
	Sensitivity 83.3%	Specificity 95%	Accuracy 90.6%	

OCT, Optical coherence tomography; RFA, radiofrequency ablation; BE, Barrett's esophagus; PPV, positive predictive value; NPV, negative predictive value.

more rigorous ablation may be required. This may involve a thorough cleaning of the ablation catheter and treatment areas to remove debris between the two sets of ablations, and if indicated, increased dosage for the RFA treatment. The ability of OCT to differentiate residual glands from normal tissue structures and debris caused by the ablation also may provide immediate information about the RFA treatment for the endoscopist. This may enable real-time evaluation of ablation depth and identification of regions requiring further treatment. The RFA treatment might be guided to further improve the efficacy of each ablation procedure. As a result, the number of treatment sessions might be reduced to reduce overall treatment time, patient anxiety, and health care cost.

Fourteen patients without dysplasia also were enrolled in this study. However, two recent large cohort studies from Northern Ireland and Denmark showed that the annual risk for adenocarcinoma in nondysplastic BE was less than 0.2%, suggesting that RFA treatment for patients with nondysplastic BE holds no benefit.<sup>32,33</sup> On the other hand, an earlier study performed in the U.S. veteran population, and perhaps better reflective of this study's population, showed a relatively higher annual risk (0.4%) for adenocarcinoma in patients with nondysplastic BE.<sup>34</sup> The National Cancer Institute estimates that the incidence of esophageal cancer in the general population of the United States (all races, both sexes, all ages) is approximately 4.5 per 100,000 (0.0045%).<sup>35</sup> Given that about 5.6% of the U.S. population is found to have BE, the incidence of esophageal cancer for patients with nondysplastic BE still appears to be much higher than in the general population.<sup>36</sup> Notwithstanding, by current clinical guidelines there is no indication for RFA treatment of patients with nondysplastic BE, and endoscopic ablation therapies are recommended mainly for patients with high-grade dysplasia.<sup>37,38</sup>

Surveillance endoscopy with biopsy is recommended for patients with low-grade dysplasia or non-dysplastic BE. However, because of the recognized limitations of the surveillance strategy, such as biopsy sampling errors, lack of compliance with surveillance protocols, cost-utility considerations, and failure to avert cancer in many cases, endoscopic therapies intended to completely remove low-

grade dysplasia and nondysplastic BE can be considered as alternative strategies.<sup>9</sup> Indeed, recent studies have shown that CE-IM can be achieved in 92% of patients with nondysplastic BE at 5-year follow-up after RFA treatment.<sup>9</sup> Although currently there is no indication to treat nondysplastic BE with RFA, in this study the BE epithelial thickness was found to be a strong predictor for RFA treatment response in all patients, both with and without dysplastic BE, indicating that this structural marker can be useful regardless of the dysplasia status of the patients.

There are several limitations in the current study. First, the study was limited to a cohort of patients with short-segment BE. This was done because the OCT system had a limited pullback imaging length, and it was desirable to image the GEJ in each data set in order to enable consistent placement of the OCT imaging catheter. Future OCT systems will be able to acquire larger data sizes, and we plan to extend the study to patients with long-segment BE and evaluate the efficacy of circumferential RFA treatment. The study also was focused on patients receiving Halo90 ablation rather than Halo360, to be consistent with the actual ablation method. In addition, the dysplasia status of the patients was evaluated before the patients went through the initial RFA treatment. As presented in Table 1, on average 2.4 and 1.7 RFA procedures were performed before the time of OCT imaging for patients in the CE-IM and non-CE-IM groups, respectively. Biopsies were generally not performed at time of RFA and OCT imaging to confirm the dysplasia status. Variations in disease severity of the patients at the time of treatment may be a confounding variable for treatment response. Future studies will be conducted to investigate the relationship between the BE mucosal thickness and treatment response in patients with different dysplasia statuses.

Second, the thickness of BE epithelium may vary if the contact pressure of the OCT catheter on the tissue changes. An ex vivo study using human colon tissues reported that the epithelium thickness was reduced when the contact pressure is increased.<sup>39</sup> This effect may induce variability in the BE thickness measurement. In the current study, the OCT catheter was in contact with the esophagus

with the endoscope at the neutral position, and the esophagus was deflated during imaging acquisition. The esophagus naturally wrapped around the OCT catheter, maintaining a consistent catheter contact for all patients. More detailed quantitative investigations are needed to understand the influence of catheter contact pressure on the BE thickness measurement.

Third, although OCT structural markers may predict RFA treatment response, the current study does not address whether RFA treatment efficacy can be improved and the number of treatments reduced by using structural information provided by 3-D OCT. A rigorous longitudinal study is needed to further establish the utility of endoscopic 3-D OCT for guiding RFA treatment of BE in clinical practice.

Finally, although the imaging coverage of the current 3-D OCT catheter is significantly larger than that of standard biopsy, a single 3-D OCT scan covered only about one-sixth of the circumference of the distal esophagus. If unburned BE or residual glands were missed by 3-D OCT immediately after RFA, the patient might fail to achieve CE-IM at follow-up even though OCT imaging may predict complete response. To overcome these potential sampling errors, multiple 3-D OCT sets will need to be acquired to achieve comprehensive coverage over different quadrants of the distal esophagus. Other OCT probe designs, such as balloon probes, also may be used to improve coverage and reduce potential sampling errors in the future.

## CONCLUSION

Endoscopic 3-D OCT can identify structural markers, including the thickness of the BE epithelium before RFA and the presence of residual glands immediately after RFA. These markers are promising predictors of RFA treatment response at follow-up in patients with short-segment BE. Three-dimensional OCT may provide valuable information that will enable endoscopists to make real-time treatment decisions improving the efficacy of RFA treatment and reducing the number of required treatments in the future.

## ACKNOWLEDGMENT

The authors acknowledge the facility support from Veterans Affairs Boston Healthcare System.

## REFERENCES

1. Odze RD, Lauwers GY. Histopathology of Barrett's esophagus after ablation and endoscopic mucosal resection therapy. *Endoscopy* 2008;40:1008-15.
2. Bergman JJ. Radiofrequency ablation—great for some or justified for many? *N Engl J Med* 2009;360:2353-5.
3. Ell C, Pech O, May A. Radiofrequency ablation in Barrett's esophagus. *New Engl J Med* 2009;361:1021; author reply 1022.
4. Shaheen NJ, Sharma P, Overholt BF, et al. Radiofrequency ablation in Barrett's esophagus with dysplasia. *N Engl J Med* 2009;360:2277-88.
5. Pouw R, Gondrie J, Sondermeijer C, et al. Eradication of Barrett esophagus with early neoplasia by radiofrequency ablation, with or without endoscopic resection. *J Gastrointest Surg* 2008;12:1627-37.
6. Dunkin B, Martinez J, Bejarano P, et al. Thin-layer ablation of human esophageal epithelium using a bipolar radiofrequency balloon device. *Surg Endosc* 2006;20:125-30.
7. Sharma VK, Wang KK, Overholt BF, et al. Balloon-based, circumferential, endoscopic radiofrequency ablation of Barrett's esophagus: 1-year follow-up of 100 patients (with video). *Gastrointest Endosc* 2007;65:185-95.
8. Shaheen NJ, Overholt BF, Sampliner RE, et al. Durability of radiofrequency ablation in Barrett's esophagus with dysplasia. *Gastroenterology* 2011;141:460-8.
9. Fleischer DE, Overholt BF, Sharma VK, et al. Endoscopic radiofrequency ablation for Barrett's esophagus: 5-year outcomes from a prospective multicenter trial. *Endoscopy* 2010;42:781,9.
10. Vaccaro B, Gonzalez S, Poneris J, et al. Detection of intestinal metaplasia after successful eradication of Barrett's esophagus with radiofrequency ablation. *Dig Dis Sci* 2011;56:1996-2000.
11. Barr H, Krasner N, Boulos PB, et al. Photodynamic therapy for colorectal cancer—a quantitative pilot-study. *Br J Surg* 1990;77:93-6.
12. Johnston MH. Cryotherapy and other newer techniques. *Gastrointest Endosc Clin N Am* 2003;13:491-504.
13. Barr H, Stone N, Rembacken B. Endoscopic therapy for Barrett's oesophagus. *Gut* 2005;54:875-84.
14. Das A, Wells C, Kim HJ, et al. An economic analysis of endoscopic ablative therapy for management of nondysplastic Barrett's esophagus. *Endoscopy* 2009;41:400, 408.
15. Inadomi JM, Somsouk M, Madanick RD, et al. A cost-utility analysis of ablative therapy for Barrett's esophagus. *Gastroenterology* 2009;136:210114.e6.
16. Huang D, Swanson EA, Lin CP, et al. Optical coherence tomography. *Science* 1991;254:1178-81.
17. Tearney GJ, Brezinski ME, Southern JF, et al. Optical biopsy in human gastrointestinal tissue using optical coherence tomography. *Am J Gastroenterol* 1997;92:1800-4.
18. Bouma BE, Tearney GJ, Compton CC, et al. High-resolution imaging of the human esophagus and stomach in vivo using optical coherence tomography. *Gastrointest Endosc* 2000;51(Pt 1):467-74.
19. Li XD, Boppart SA, Van Dam J, et al. Optical coherence tomography: advanced technology for the endoscopic imaging of Barrett's esophagus. *Endoscopy* 2000;32:921-30.
20. Poneris JM. Diagnosis of Barrett's esophagus using optical coherence tomography. *Gastrointest Endosc Clin N Am* 2004;14:573-88.
21. Evans JA, Nishioka NS. The use of optical coherence tomography in screening and surveillance of Barrett's esophagus. *Clin Gastroenterol Hepatol* 2005;3:S8-11.
22. Chen Y, Aguirre AD, Hsiung PL, et al. Ultrahigh resolution optical coherence tomography of Barrett's esophagus: preliminary descriptive clinical study correlating images with histology. *Endoscopy* 2007;39:599-605.
23. Adler DC, Zhou C, Tsai TH, et al. Three-dimensional optical coherence tomography of Barrett's esophagus and buried glands beneath neosquamous epithelium following radiofrequency ablation. *Endoscopy* 2009;41:773-6.



24. Suter MJ, Vakoc BJ, Yachimski PS, et al. Comprehensive microscopy of the esophagus in human patients with optical frequency domain imaging. *Gastrointest Endosc* 2008;68:745-53.
25. Adler DC, Zhou C, Tsai TH, et al. Three-dimensional endomicroscopy of the human colon using optical coherence tomography. *Optics Express* 2009;17:784-96.
26. Zhou C, Adler DC, Becker L, et al. Effective treatment of chronic radiation proctitis using radiofrequency ablation. *Ther Adv Gastroenterol* 2009;2:149-56.
27. Isenberg G, Sivak MV, Chak A, et al. Accuracy of endoscopic optical coherence tomography in the detection of dysplasia in Barrett's esophagus: a prospective, double-blinded study. *Gastrointest Endosc* 2005;62:825-31.
28. Zhou C, Tsai TH, Lee HC, et al. Characterization of buried glands pre- and post-radiofrequency ablation using three dimensional optical coherence tomography. *Gastrointest Endosc*. Epub 2012 Apr 4.
29. Sharma P, Dent J, Armstrong D, et al. The development and validation of an endoscopic grading system for Barrett's esophagus: The Prague C & M Criteria. *Gastroenterology* 2006;131:1392-9.
30. Adler DC, Chen Y, Huber R, et al. Three-dimensional endomicroscopy using optical coherence tomography. *Nature Photonics* 2007;1:709-16.
31. Trunzo J, McGee M, Poulouse B, et al. A feasibility and dosimetric evaluation of endoscopic radiofrequency ablation for human colonic and rectal epithelium in a treat and resect trial. *Surgical Endoscopy* 2011;25:491-6.
32. Bhat S, Coleman HG, Yousef F, et al. Risk of malignant progression in Barrett's esophagus patients: results from a large population-based study. *J Natl Cancer Inst* 2011;103:1049-57.
33. Hvid-Jensen F, Pedersen L, Drewes ArM, et al. Incidence of adenocarcinoma among patients with Barrett's esophagus. *New Engl J Med* 2011;365:1375-83.
34. Spechler SJ, Lee E, Ahnen D, et al. Long-term outcome of medical and surgical therapies for gastroesophageal reflux disease—follow-up of a randomized controlled trial. *JAMA* 2001;285:2331-8.
35. Howlader N, Noone NA, Krapcho M, et al, (eds). SEER Cancer Statistics Review, 1975-2009 (Vintage 2009 Populations). National Cancer Institute. Bethesda, MD, [http://seer.cancer.gov/csr/1975\\_2009\\_pops09/](http://seer.cancer.gov/csr/1975_2009_pops09/), based on November 2011 SEER data submission, posted to the SEER Web site, April 2012.
36. Hayeck TJ, Kong CY, Spechler SJ, et al. The prevalence of Barrett's esophagus in the US: estimates from a simulation model confirmed by SEER data. *Dis Esophagus* 2010;23:451-7.
37. Wang KK, Sampliner RE. Updated Guidelines 2008 for the diagnosis, surveillance and therapy of Barrett's esophagus. *Am J Gastroenterol* 2008;103:788-97.
38. Spechler SJ, Sharma P, Souza RF, et al. American Gastroenterological Association technical review on the management of Barrett's esophagus. *Gastroenterology* 2011;140:e18-e52.
39. Westphal V, Rollins AM, Willis J, et al. Correlation of endoscopic optical coherence tomography with histology in the lower GI tract. *Gastrointest Endosc* 2005;61:537-46.

*Abbreviations:* BE, Barrett's esophagus; CE-D, complete eradication of dysplasia; CE-IM, complete eradication of intestinal metaplasia; GEJ, gastroesophageal junction; OCT, optical coherence tomography; RFA, radiofrequency ablation; 3-D, three-dimensional



**This video can be viewed directly from the GIE website or by using the QR code and your mobile device. Download a free QR code scanner by searching "QR Scanner" in your mobile device's app store.**

**DISCLOSURE:** This work was supported by the Massachusetts Institute of Technology(MIT)/CIMIT Medical Engineering Fellowship (T.H.T.), the Veterans Affairs Boston Healthcare System, NIH grants R01-CA75289-15 (J.G.F. and H.M.), R44CA101067-06 (J.G.F.), and K99-EB010071-01A1 (C.Z.), Air Force Office of Scientific Research grant FA9550-10-1-0063 (J.G.F.) and Medical Free Electron Laser Program grant FA9550-10-1-0551 (J.G.F.). D. Adler and J. Schmitt are full-time employees of Lightlab Imaging Inc, St. Jude Medical. J. Fujimoto receives royalties from intellectual property owned by MIT and licensed to Lightlab Imaging Inc, St. Jude Medical and royalties from intellectual property owned by MIT and licensed to Carl Zeiss Meditec and is a scientific advisor for and has stock options with Optovue, Inc. No other financial relationships relevant to this publication were disclosed.

Copyright © 2012 by the American Society for Gastrointestinal Endoscopy  
0016-5107/\$36.00  
<http://dx.doi.org/10.1016/j.gie.2012.05.024>

Received February 29, 2012. Accepted May 17, 2012.

Current affiliations: Department of Electrical Engineering & Computer Science (1), Research Laboratory of Electronics, Massachusetts Institute of Technology, Cambridge; Veterans Affairs Boston Healthcare System (2), Harvard Medical School (3), Boston; LightLab Imaging Inc (4), St. Jude Medical Inc, Westford, Massachusetts, USA.

Reprint requests: Hiroshi Mashimo, MD, PhD, Gastroenterology Section, Veterans Affairs Boston Healthcare System, Harvard School of Medicine, Boston, MA 02130.

If you would like to chat with an author of this article, you may contact Dr Mashimo at [hmashimo@hms.harvard.edu](mailto:hmashimo@hms.harvard.edu).

### GIE on Twitter

GIE now has a Twitter account. Followers will learn when the new issues are posted and will receive up-to-the-minute news as well as links to author interviews, podcasts, and articles. Search on Twitter for @GIE\_Journal and follow all of GIE's tweets.